

# A morphological fusion algorithm for optical detection and quantification of decay patterns on stone surfaces

P. Kapsalas <sup>a</sup>, P. Maravelaki-Kalaitzaki <sup>b</sup>, M. Zervakis <sup>a</sup>, E.T. Delegou <sup>c</sup>, A. Moropoulou <sup>c,\*</sup>

<sup>a</sup> *Technical University of Crete, Department of Electronics and Computer Engineering, Chania 73100, Greece*

<sup>b</sup> *Ministry of Culture, 25th Ephorate of Prehistoric and Classical Antiquities, Chania 73100, Greece*

<sup>c</sup> *National Technical University of Athens, School of Chemical Engineering, Athens 15780, Greece*

Received 28 June 2006; received in revised form 1 August 2006; accepted 10 August 2006

Available online 27 October 2006

## Abstract

The quantification of black crust formation on exposed stone has been carried out in this work with the aid of non-destructive analytical techniques. The proposed non-destructive Morphologically Fused Detection (MFD) approach, quantifies the deterioration effects encountered on marble surfaces by providing the number, location and shape of deterioration spots. According to this approach, a weighted difference of Gaussians filter determines the exact locations of deterioration patterns, a morphological detector provides the shape of such patterns and finally a conditional thickening operator combines location and shape information from the previous stages. The detected decay areas are segmented and distinguished into white and black spots according to their chemical composition. Besides applications in assessing deterioration and monitoring the decay rate of exposed stone with time, MFD can be further employed for evaluating the efficiency of cleaning methods. The algorithm is tested on a large set of images depicting a variety of degradation effects. The derived results are in accordance with assessments obtained by chemical analyses.

© 2006 Elsevier Ltd. All rights reserved.

*Keywords:* Stone decay diagnosis; Chemical cleaning evaluation; Optical inspection; Morphological operations; Blob analysis; Statistical evaluation

## 1. Introduction

Natural weathering and human activities induce changes in air quality and subsequent effects on building materials [1]. Airborne pollutants affect buildings by forming black crusts on sheltered surfaces [2]. The most frequently encountered chemical constituents in black crusts are gypsum, calcite, silicates, potassium nitrate, metal oxides and numerous organic constituents in low concentration [3]. Black crusts, ranging in thickness from 100  $\mu\text{m}$  up to several mm, not only affect the aesthetic view of monuments, but also lead to further erosion due to the catalyzing action of the crust components [3]. Observations of thin sections of crusts under a polarizing microscope reveal that sporadic small black particles are responsible for the

coloration of the crust, while white particles are mainly associated with the presence of gypsum crystals and re-crystallized  $\text{CaCO}_3$ . Chemical cleaning of crusts becomes essential not only for the conservation of the deteriorated areas, but also for preventing further erosion phenomena. In order to select the most appropriate cleaning method, the key step is an effective diagnostic process capable of defining the decay patterns, as well as the extent and thickness of the eroded areas. The diagnostic processes used so far are mainly destructive, involving removal of a specimen from the stone and subsequent chemical analysis. The development of non-destructive methods capable of performing reliable detection and quantification of the deterioration patterns is currently an issue under investigation.

Image Processing (IP) techniques can be used for extracting information regarding the eroded areas in artworks, as indicated by previous works [4–8]. However, the investigation of such approaches is still in early stages.

\* Corresponding author. Tel.: +30 210 7723276/1433.

E-mail address: [amoropul@central.ntua.gr](mailto:amoropul@central.ntua.gr) (A. Moropoulou).

A survey of methods for quantifying the color alteration induced by weathering was conducted by Lebrun [4]. Pappas and Pitas [5] employed IP methods for the conservation of old paintings with the aim of diagnosing the deterioration effects and performing digital restoration. IP approaches were also applied to back-scattered electron images obtained with scanning electron microscopy-energy dispersive X-rays analysis to identify and quantify salts and porosity with depth in porous media [6]. Furthermore, methods for characterizing the stone structure and detecting regions of material loss were developed in the study of Moltedo et al. [7]. Finally Boukouvalas et al. [8] introduce computer vision techniques for the detection and classification of mineral veins encountered on ceramic tiles surfaces.

The objective of this paper is to investigate and assess the potential of microscopic optical inspection via IP techniques in nondestructive qualitative and quantitative evaluation of degradation patterns on marble surfaces. The paper introduces a computer-aided method for analysis of black and white particles observed on exposed marble decay areas. The employed approach, referred to as “Morphologically Fused Detection (MFD)”, combines operators that have been successfully applied to mammographic image analysis, an area that poses similar peculiarities in both the structure of spots to be detected and the appearance of the background [9]. Similar algorithmic processes have been extensively applied to other medical applications, such as macular degeneration and analysis of Computerized Tomography Magnetic Resonance Images (CT/MRI), with considerable success [9,10].

The design of an effective detection scheme should thoroughly consider the peculiarities of the problem under consideration. Thus, an important concept is the reduction of false positive and false negative rates, which is partially achieved by detecting decay areas at their real extent. Shape preservation is also an important aspect. The MFD approach makes use of the knowledge of the approximate size of spots, their spatial arrangement and their expected shape, thus utilizing a better understanding of the size and morphology of corrosion patterns. The precise knowledge of these attributes, however, is not crucial. To attain the desirable performance, we employ a multi-stage algorithm [11,12] for the estimation of location and rough extent of decay areas (providing qualitative measures) and the morphological analysis in terms of the shape of these areas (deriving quantitative measures). More specifically, our approach considers a weighted difference of Gaussians filter to determine the exact locations of prevalence of deterioration patterns and a morphological filtering process to derive more accurate shape information for such spots of deterioration. The results of both detectors are fused through a conditional thickening operator with the aim of deriving both accurate location and shape information. Finally, the distinguished dark and bright spots are segmented to provide

local intensity measurements related to the depth of deterioration. Among the robust points of the MFD approach, we consider its potential to fuse segmentation results derived by two independent detectors, each focusing on specific attributes of corrosion including shape, topology and size characteristics. Other alternative histogram-based or region-based detection schemes on micro-scale images have the substantial drawback of ignoring information regarding the spatial distribution of intensity values. A further significant characteristic of our detection methodology is its fast speed in performing segmentation. All its computations are of linear complexity, enabling future applications of the algorithm as a detection tool within an integrated information system.

The algorithm is applied to images obtained with the Fiber Optics Microscope (FOM) depicting a variety of degradation patterns. Due to the quite general specifications employed in its design, the proposed algorithm can be applied for the evaluation of decay areas formed on a broad range of background surfaces. Consistent monitoring of these effects in the course of time can reveal valuable information regarding the environmental effects on materials and structures. Besides its applicability on assessing the extent of deterioration effects on exposed surfaces, it can also be used to compare the effectiveness of cleaning methods by assessing the remaining degradation effects after cleaning. The algorithmic results provide consistent conclusions, which are also in accordance with assessments from chemical analysis of the surface material [13,14].

## 2. Problem specifications

### 2.1. Experimental setup

The studied surfaces were located on flutings and reedings from columns of the National Archaeological Museum of Athens, Greece. The fluting FOM images represent areas sheltered from rain action, while reeding FOM images depict areas unsheltered from rain action. It is observed that sheltered stone surfaces develop crusts more extensively, as well as thicker and darker in color, than those observed on unsheltered areas. The rain-washed areas are characterized by dissolution effects and flaking of the stone, as a result of the continuous rain and wind action. Flutings function as cavities where pollutants and airborne particles (fly ash, metal oxides, carbonate particles, dust, etc) are deposited, while reedings accumulate fewer pollutants due to the washing effect of the rain. This discrimination was also reflected in the FOM images depicting flutings and reedings even from the same column. Figs. 1a and b illustrate sheltered and unsheltered marble surfaces, respectively, as observed under the FOM monitoring system.

FTIR and SEM-EDS analyses revealed that black crusts on flutings consist of an external, 30  $\mu\text{m}$  thick, layer of macrocrystalline gypsum mixed with aluminosilicates, calcite, nitrates and oxalates. Another successive internal

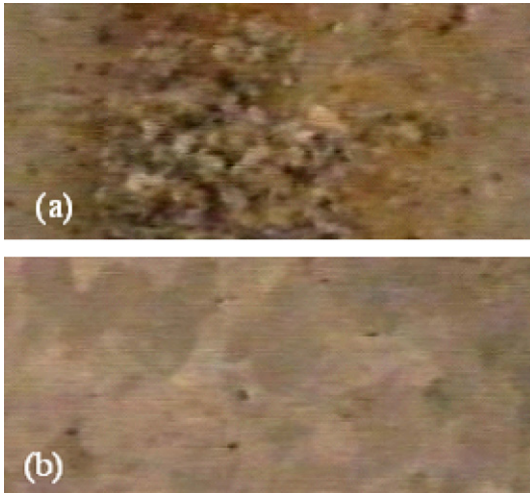


Fig. 1. Black and white particles on a stone surface: (a) sheltered and (b) unsheltered from the rain action as observed under the Fiber Optic Microscope (FOM).

layer, 40  $\mu\text{m}$  thick, was also observed and consisted of microcrystalline gypsum and calcite [13]. The crusts on sheltered readings comprise calcite and lower quantity of gypsum than the corresponding ones on flutings [14].

The applied cleaning interventions on the investigated marble surfaces were an ion-exchange resin paste with deionized water (DS), a biological paste (BP) of 1000 ml deionized water, 50 g  $(\text{NH}_2)_2\text{CO}$ , 20 ml  $(\text{CH}_2\text{OH})_2\text{CHOH}$  and approximately 800 g sepiolite, and a Wet Microblasting Method (WMB) springing spherical particles of calcium carbonate, with diameter lower than 80  $\mu\text{m}$ , with a maximum function pressure of 0.5 bar. The proportion of water and spherical particles of calcium carbonate in the device's commixture barrel was 3:1. The cleaning performance was assessed by chemical investigations of the cleaned surfaces with the aid of destructive techniques. The results of the chemical analysis are subsequently used to compare the efficiency of the employed cleaning techniques and to estimate the accuracy of the automated approach.

Aiming at assessing the efficiency and accuracy of the chemical cleaning methods in a non-destructive way, FOM images before and after chemical cleaning are analyzed by the proposed algorithmic scheme (MFD). In this study, the decay patterns are discriminated into two broad categories: "black particles" and "white particles". "Black particles" are associated with the presence of carbonaceous particles, alumino-silicates, dust, metal oxides and other pollutants embedded in the gypsum cavities. On the other hand, "white particles" represent decay patterns associated with gypsum crystals and re-crystallized  $\text{CaCO}_3$ . The degree of decay and the efficiency of the chemical cleaning methods are assessed by considering the number and location of black and white particles, as well as their extent and thickness. An overall parameter to assess the degradation state is the percentage of the marble surface covered by decayed areas.

## 2.2. Requirements for effective detection and segmentation

Aiming at the design of an efficient detection process, we initially consider the peculiarities of the problem and the features (geological and other) of decay areas. In this study, FOM images from marble surfaces exposed to the rain action provide the geological characteristics to be considered as reference material in the detection process. Prior researches on the potential of the FOM monitoring system [15] verified its ability to distinguish different substrates, e.g. marble from porous limestones, decay patterns prevailing on areas of different exposure and surfaces treated by different cleaning procedures. Furthermore, it provides a quite effective screening of irregularities associated with the stone structure and the depth of deterioration.

Given a FOM image, there are three major problems in analyzing decay patterns' attributes.

- The black (white) particles are small in extent and they are visible as dark (bright) spots in an inhomogeneous background.
- The deterioration patterns are located on inhomogeneous background that often reflects the structure of the marble surface. As a consequence, the local background of the image may be brighter than some "white particles" located in other parts of the same image. Thus, for detecting and determining the exact location of black and white particles in an image, a detection process should be based on local rather than global characteristics of the image.
- Another feature encountered on the studied images is the typically low contrast between the small deterioration patterns and the background; the latter often reflects similar variation of the intensity to noise variation appearing on the inhomogeneous marble structure. Our aim is to design a method as sensitive as possible to systematic variations caused by deterioration patterns, while suppressing those random variations due to noise. Thus, our segmentation process should be dynamic as to take into account the local intensity variations.

These image characteristics should guide the design of an effective particle detector, able to overcome several limitations of conventional detectors on the problem under consideration. More specifically our detector is designed based on the following properties:

- It should be insensitive to large-scale background intensity variations, which are characterized by low spatial frequencies.
- It should be adaptive to the noise level within a neighborhood. Spots of high contrast should be detected even within an area of high noise levels, whereas spots of low contrast should be located in all background areas.
- Since the nominal size of spots is approximately known but may vary, the detector should be adapted to spot sizes in the region of an expected value. A prior

assumption about the shape of the spots is that they are round, favoring the use of an angular isotropic operator.

### 3. Proposed approach for detection of decay areas

The detection process aims to derive both coverage (percentage of area covered by spots) and morphological (number and exact area of spots) measures regarding decay areas. Thus, it addresses both accurate location estimation and efficient shape segmentation. In order to achieve these objectives operating on a locally varying background that often characterizes the marble surface, the proposed approach is adaptive and combines several operators, each focusing on a particular objective. Its major components involve a Gaussian detector appropriate for location estimation and a morphological filter that allows more accurate shape estimation. The combination of the results of these two detectors via a conditional thickening operator guarantees low false-positive rate in detection and preserves shape attributes of the detected areas.

#### 3.1. Gaussian detector

The specifications of segmentation in Section 2.2 are employed in the design of our corrosion spot detector. The first step towards the implementation of such an efficient spot detector is to decouple the detection of useful information from the background activity. Thus, the Gaussian detector proceeds by initially employing a broadband highpass filter for the extraction of intensity variations and a subsequent thresholding scheme for the isolation of structures related to decay spots. Each stage involves both global and local processing for most effective detection of abnormal formations (spots) on an inhomogeneous background.

The filtering stage is based on the Difference of Gaussians (DoG) scheme, which implements the subtraction of one smoothed version of the image from another version expressing a different degree of smoothing [11]. In global consideration, the DoG filtering extracts a smooth background from the original image preserving only intensity variation that can be attributed to abnormal structures. The original image  $f(x, y)$  is processed as:

$$f_1(x, y) = f(x, y) - G_4[f(x, y)], \quad (1)$$

where the Gaussian kernel  $G[\cdot]$  is chosen with standard deviation  $\sigma = 4$  as to reflect the expected dimensions of the black and white particles and the inter-particle distance. This means that spatial variations at a scale larger than this are attenuated. In this way, the smoothing process realized by the Gaussian filtering does not affect information at the scale of interest. More specifically, prior SEM-EDS analyses of black crusts provide information on the size of decay patterns. Such analyses reveal that the decay patterns exhibit a diameter ranging from 10 up to 150  $\mu\text{m}$

and shape that does not deviate significantly from the circle [16,17]. These attributes are considered in the selection of the filters' variation parameters and the size of the filters' window, so that filtering and interpolation does not affect the extent or the spatial distribution of the areas of interest. After the acquisition of image  $f_1$  (detail image), local processing attempts to derive spots of small contrast over the local background. The weighted DoG operator is now employed, using two kernels of standard deviation  $\sigma_1 = 0.25$  and  $\sigma_2 = 6$ , respectively, as to suppress very small structures (via  $\sigma_1$ ) and slowly varying intensity patterns (via  $\sigma_2$ ). The application of the two kernels is in reverse order in the detection of black and white particles and operates as follows, for black particle detection:

$$f_2(x, y) = w_1 \times G_6[f_1(x, y)] - G_{0.25}[f_1(x, y)] \quad (2)$$

and for white particle detection:

$$f'_2(x, y) = w_2 \times G_{0.25}[f_1(x, y)] - G_6[f_1(x, y)] \quad (3)$$

Thus, for a black spot to be detected, the local average defined by the kernel of size  $\sigma_6$  ( $\sigma_{0.25}$  for white spots) has to be larger than in a factor  $\frac{1}{w_1}$  from the local average defined by the kernel of size  $\sigma_{0.25}$  ( $\sigma_6$  respectively). The important point of this criterion is that the detection process becomes invariant with respect to the relative intensity scale of structures within  $f_1(x, y)$ . This means that a low contrast spot in a homogeneous background is detected equally well as a high contrast spot in an area of a high noise level. Based on the geological characteristics of the substrate and the decay patterns, this value is set to  $w_1 = 0.8$  ( $w_2 = 0.6$ ).

Following the filtering stage, the detection of black and/or white spots from the DoG image  $f_2(x, y)$  proceeds on the basis of a twin thresholding scheme on the histogram of  $f_2(x, y)$ . The first threshold equal to  $k_1$  times the standard deviation of the histogram is applied to  $f_2(x, y)$ . Subsequently, the standard deviation is re-calculated using only the pixels above the initial threshold. The second threshold is set at  $k_2$  times the recalculated standard deviation. Methods for selecting the parameters  $k_1$  and  $k_2$  are reported in [18]. In our application  $k_1 = k_2 = 1.5$  for the detection of white spots, while for the detection of black spots  $k_1$  and  $k_2$  are set to 2 and 3, respectively.

#### 3.2. Morphological filtering

The Gaussian detector is capable of detecting the topology of deterioration patterns, but distorts their shape; the boundary of individual spots is over-smoothed. For enabling further analysis on corrosion damage type and attributes however, it is essential to derive accurate shape information of the derived areas. Shape is preserved by a morphological detector [12], operating in parallel with the Gaussian detector in two stages, i.e. filtering and thresholding. Filtering is based on combinations of the two fundamental morphological operations, namely erosion ( $M \ominus B$ ) and dilation ( $M \oplus B$ ) for an image  $B(x, y)$  and a structuring element

$M(x, y)$ , respectively. A disk-shaped structuring element of a radius equal to 11 pixels is employed in our application, since the deterioration patterns of interest are considered approximately round in shape. The dilation operation tends to eliminate or reduce dark details, while erosion removes bright details of an image, depending on the size and shape of the structuring element.

By combining erosion and dilation, the important morphological operations of opening [ $M \circ B := M \ominus (M \oplus B)$ ] and closing [ $M \bullet B := M \oplus (M \ominus B)$ ] are obtained. Furthermore, based on these operators, the top-hat and bot-hat transforms of an image are defined as:

$$R := B - (M \circ B) \tag{4}$$

$$R := B - (M \bullet B) \tag{5}$$

respectively. The bot-hat (top-hat) transform enhances dark (bright) particles that have sizes smaller than the structuring element  $M$ . Following these highpass filtering schemes, the detection process is based on a twin thresholding process, similar to that of the Gaussian detector.

### 3.3. Conditional thickening and the proposed MFD approach

At this stage we attempt to combine the results of the previous methods as to derive accurate information regarding the number, location and shape of the spots. For this purpose, the conditional thickening operator denoted by  $\otimes$  is applied on a spot  $X$  relative to  $Y$  with the pair of structuring elements  $(M_{i1}, M_{i2})$  as follows [12]:

$$(M_{i1}, M_{i2}) \otimes XY = Y \cap (X \cup ((M_{i1} \ominus X) \cap (M_{i2} \ominus X^C))) \tag{6}$$

More specifically, a spot  $X$  of the Gaussian detector is expanding up to the point that it reaches a neighbouring spot or until it reaches the size of a co-located spot  $Y$  detected by the morphological operator. The pair of structuring elements  $M_{i1}$  and  $M_{i2}$  controls the direction of expansion. To cover spatial expansion in many directions, we use eight pairs of such elements for either black or white spots. The first two pairs are given as:

$$(M_{11}, M_{12}) = \left( \begin{bmatrix} 1 & 1 & 1 \\ 0 & 0 & 0 \\ 0 & 0 & 0 \end{bmatrix}, \begin{bmatrix} 0 & 0 & 0 \\ 0 & 1 & 0 \\ 1 & 1 & 1 \end{bmatrix} \right) \text{ and}$$

$$(M_{21}, M_{22}) = \left( \begin{bmatrix} 0 & 0 & 0 \\ 0 & 0 & 1 \\ 0 & 1 & 1 \end{bmatrix}, \begin{bmatrix} 0 & 0 & 0 \\ 1 & 1 & 0 \\ 0 & 1 & 1 \end{bmatrix} \right)$$

The remaining pairs are obtained from these matrix combinations through rotations every  $90^\circ$ . Finally, the conditional thickening operator is obtained as a combination of individual results for every pair  $(M_{i1}, M_{i2})$ :

$$E = \bigcup_{i=1}^8 (M_{i1} M_{i2}) \otimes XY \tag{7}$$

The operator in Eq. (7) defines the MFD approach, which employs the conditional thickening operator to combine and fuse the results of two individual detectors. The conditional thickening equation is applied with initial condition  $E = X$ , the result of the Gaussian detector, and iterates towards  $Y$ , the result of the morphological detector, until  $E$  does not change any further. An example case of the detection process is presented in Fig. 2. A particularly useful property of this operator is that either  $X$  increases until the boundaries of  $Y$  are reached, or until two subsets of  $X$  are separated by a space of one pixel in width. Consequently,  $E$  is always a subset of  $Y$  and contains as many objects as the intersection of  $X$  and  $Y$ . For the decay areas, this means that the patterns detected by the Gaussian detector (Fig. 2a) are extended in space but the result is always intersected with the spots detected by the morphological detector (Fig. 2b). The intersection in each step preserves only spots collocated in both  $X$  (after conditional thickening) and  $Y$ . An illustration of the MFD's operation is provided in Fig. 3.

In summary the proposed MFD approach involves application of the Gaussian and morphological detectors in parallel and combination of their results through conditional thickening. This approach approximates quite accurately the shape and size of dark and/or bright crusts and provides reliable information about their topology. The results obtained on a variety of images from marble surfaces support the effectiveness of the MFD approach as a diagnostic tool for the study of deterioration patterns. In order to further proceed with quantitative measurements, the detected patterns are segmented into masks of compact areas and are labeled. This process provides information regarding the number and size of decay areas that can be used in statistical analysis of the decay phenomena. Furthermore, the segmented masks overlaid on the original image provide intensity information for the decay areas that can lead to conclusions about the depth of degradation/erosion on the surface inspected. Such studies relating intensity information to severity of degradation are cur-

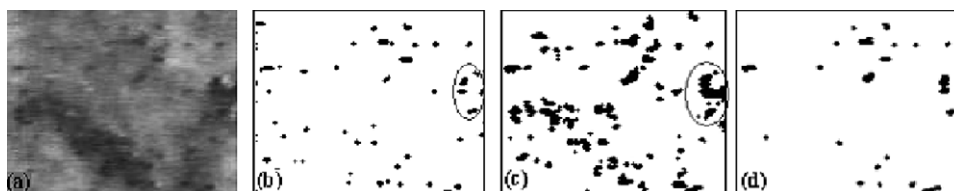


Fig. 2. (a) A reeding located on sheltered areas as it is monitored by the FOM; black particles detected by: (b) the Gaussian detector algorithm, (c) the morphological filtering operations, and (d) the proposed MFD approach.

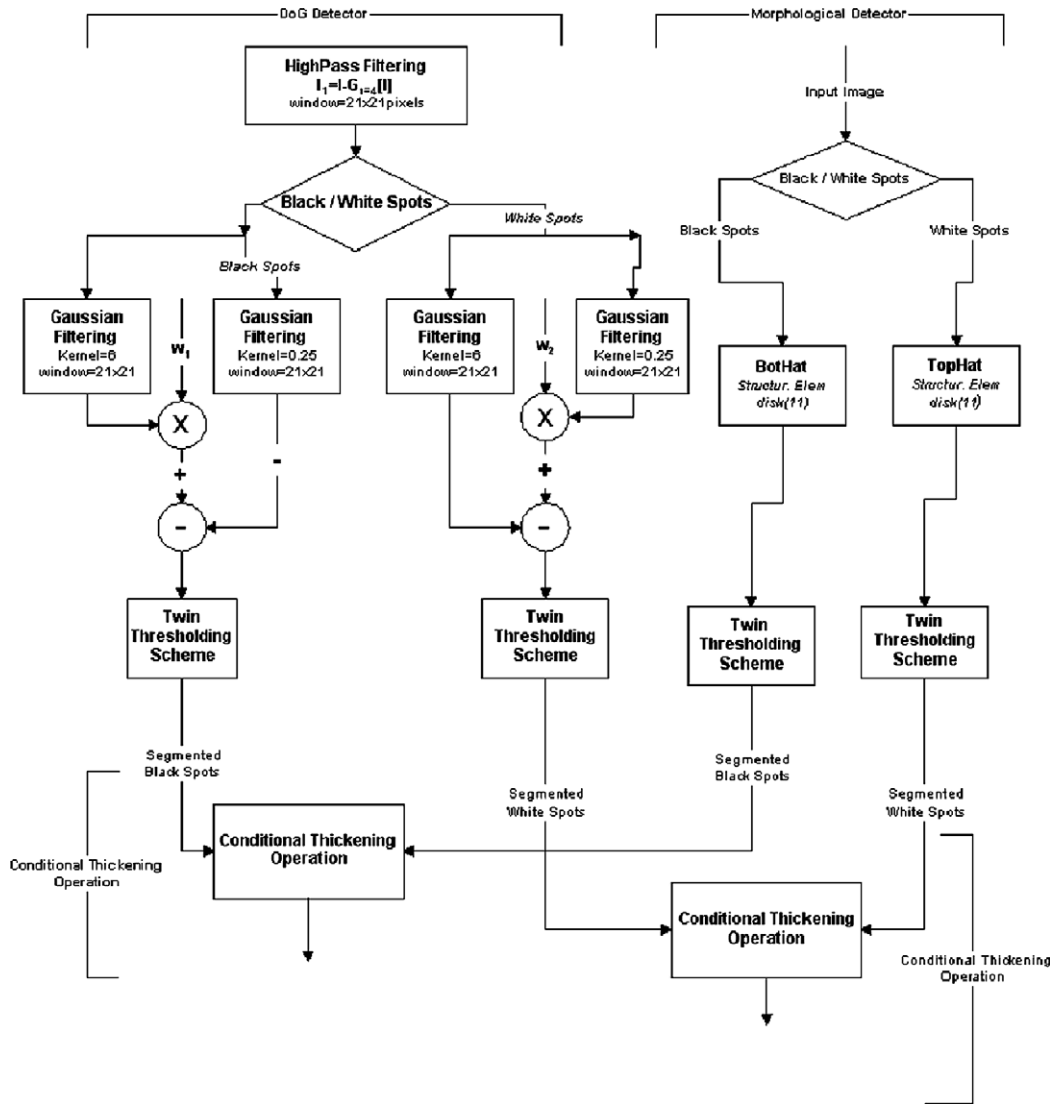


Fig. 3. A flowchart of the MFD approach.

rently under investigation. The evaluation of the MFD approach for the problem under consideration is presented in the next section via several examples illustrating its performance.

#### 4. Results and discussion

Our evaluation of the MFD approach is performed by both qualitative and quantitative means. Qualitative evaluation is assessed through experts, by optically inspecting the original images and the detection results. The above analysis is essential for estimating the correctness of the detected deteriorated areas concerning their location and size or shape characteristics. The automated approach discussed in this paper is tested on a set of 25 images depicting marble surfaces prior and after any chemical cleaning treatment. In the following tables summarizing our results, the untreated images are denoted by “diagnosis”, whereas the treated images are denoted by the cleaning method as DS,

BP, or WMB. The statistical (quantitative) measures computed from the detected areas, exemplify the effectiveness of this approach in quantifying the deterioration state. The images studied with our algorithmic approach are obtained with the same specifications in terms of the resolution of the FOM, the horizontal and vertical dimensions and the duration of exposure of the original stone regions to weathering. Such similarity of features is of high significance as it guarantees the comparability of the obtained results.

##### 4.1. Qualitative results

This section presents and discusses several results obtained, demonstrating the performance of the MFD approach. Fig. 4 depicts a black crust located on a sheltered fluting (a), while (b) and (c) illustrate the black and white particles, respectively, as detected by the MFD algorithm. It is readily observed that this algorithm sufficiently



Fig. 4. (a) Sub-area of an untreated black crust located on fluting at sheltered areas, (b) white and (c) black particles detected by the MFD Algorithm.

distinguishes the deterioration patterns related to the presence of black and white particles. According to the experts, the detected areas (number and size) are in good accordance with their own judgment of deterioration patterns prevalence in the image. Even the sporadic distribution of small black particles observed on polished sections of black crusts corresponds to the spatial arrangement of decay patterns segmented by MFD [13,14,17]. The results of the algorithm on FOM images after chemical cleaning are illustrated in the next figures. More specifically, Fig. 5 illustrates part of the surface located on a sheltered fluting cleaned with the BP method. The cleaned surfaces are located in adjacent areas to the untreated black crust illustrated in Fig. 4. By comparing the above figures it becomes evident that the deterioration effects are eliminated after the application of chemical cleaning methods. Thus, the white and black particles detected on the untreated surface (Figs. 4a and b) are more in number and larger in size than those of the cleaned surfaces (Fig. 5). This analysis assesses in a qualitative way the effectiveness of the applied chemical cleaning methods.

The proposed algorithm was also applied to the study of an interface partially cleaned with the WMB method (Fig. 6). In this case, the algorithmic process is applied to the same homogeneous structure before and after cleaning and provides a test-bed for comparative results under the

same structural conditions. Fig. 6a depicts a compact piece of marble as observed under FOM, where the lower part is cleaned and the upper part represents the untreated surface. The red line defines the boundary between treated and untreated surface. Because of the spatial proximity of the two areas, it can be assumed that the density, size and spatial distribution of the original deterioration patterns were comparable. Thus, comparisons on the two regions really reflect comparisons on the same area before and after treatment. This setup allows immediate qualitative and quantitative conclusions regarding the effectiveness of the MFD algorithm to assess the effects of cleaning. The results of the MFD process in terms of black and white particles are shown in Fig. 6b and c, respectively. Optical inspection on Figs. 6b and c by the experts verifies that the spatial distribution of the detected deterioration patterns closely resembles their own judgment of sporadic particle presence. The differences in the spots detected above and below the red line is obvious, reflecting the significant removal of degradation effects by the chemical cleaning.

The results presented so far are in accordance with the expected pollutant removal induced by the chemical cleaning methods. From these examples, it becomes obvious that application areas of the proposed method include: (1) the evaluation of the decay effects on marble surfaces, (2) the tracking of decay over time as a means of evaluating



Fig. 5. (a) Sub-region of an image illustrating a sheltered fluting cleaned by the Biological Paste method (BP), (b) white and (c) black particles detected by the MFD algorithm.

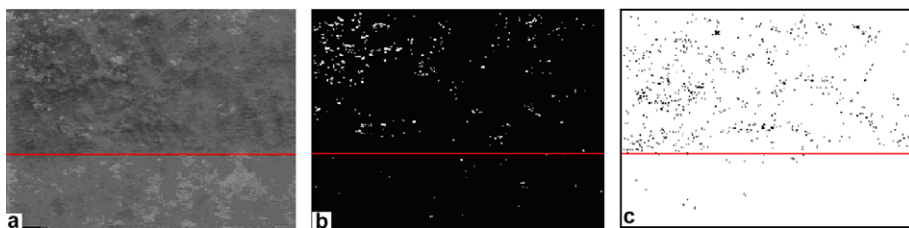


Fig. 6. (a) Marble surface located on an unsheltered fluting; (b) white (c) and black particles detected by the MFD approach in the un-cleaned (above the red line) and cleaned area (below the red line). The areas above and below the red line illustrate the degradation states before and after WMB cleaning. (For interpretation of the references in colour in this figure legend, the reader is referred to the web version of this article.)

environmental effects, (3) the assessment of the effects of a cleaning method on the marble surface and (4) the ability to compare the performance of several cleaning methods, as far as removal of black and white particles is concerned.

4.2. Quantitative results

The images studied by the MFD algorithm are quantified by measuring the number of spots, the percentage of area covered by such spots and their average size and spatial distribution. In order to increase the reliability of statistical measures concerning the spatial distribution of spots prior and after cleaning, we adopt a consideration on many image sub-regions. More specifically, each image depicting the decay state on stone surfaces is segmented to nine sub-areas of equal dimensions. Subsequently, the number of deterioration patterns in each of the sub-areas is computed and used to obtain a mean number of decay patterns per sub-area. Table 1 depicts the mean number of black and white particles (along with its standard deviation) detected on sheltered and unsheltered surfaces before and after cleaning (total 25 images sectioned in sub-areas as before),

as well as on the interface of an untreated and a WMB cleaned area depicted in Fig. 6. The measurement area corresponds to 1/9th of the FOM image size, corresponding 25.389 mm<sup>2</sup> of the original stone surface.

Several conclusions can be drawn from the results of Table 1, where the chemical composition of the various cases of interest is also indicated as derived by chemical analysis. The mean number of either black or white particles is significantly reduced after chemical cleaning. Sheltered surfaces and flutings show more decay patterns than unsheltered surfaces and reedings. These results can reasonably well be interpreted by the fact that sheltered areas and column flutings accumulate the atmospheric deposition, as expressed by the higher amount of aluminosilicates and gypsum identified. Unsheltered areas and column reedings, being more exposed to rain and wind action, show lower amount of decay products.

The qualitative (visual) and quantitative measures extracted from the MFD analysis can further be used to assess the capability of the chemical intervention methods. Interpreting the results of Table 1, it is concluded that the DS method (anionic resin with de-ionized water) is less

Table 1

Mean number of black (B-P) and white (W-P) particles located on the untreated (diagnosis) and cleaned surfaces (DS, BP, WMB) (the standard deviation (std) is reported in parenthesis)

	Diagnosis <sup>1</sup>		DS <sup>2</sup>		BP <sup>3</sup>		WMB <sup>4</sup>	
	B-P	W-P	B-P	W-P	B-P	W-P	B-P	W-P
Sheltered flutings	94.86 (6.17)	50.42 (3.58)	8.44 (1.91)	1.11 (0.46)	3.55 (0.32)	3.77 (1.18)	2.11 (0.46)	0.44 (0.11)
Sheltered flutings chemical analysis	Gypsum <sup>b</sup> , calcite <sup>c</sup> , aluminosilicates <sup>d</sup> , nitrates <sup>e</sup> , oxalates <sup>e</sup>		Calcite <sup>a</sup> , gypsum <sup>e</sup> , oxalates <sup>e</sup> , aluminosilicates <sup>f</sup>		Calcite <sup>a</sup> , oxalates <sup>e</sup> , gypsum <sup>e</sup>		Calcite <sup>a</sup> , oxalates <sup>e</sup> , gypsum <sup>f</sup>	
Sheltered reedings	47.44 (2.60)	12.33 (2.82)	0.99 (0.33)	0.77 (0.51)	0.67 (0.35)	0.33 (0.22)		
Sheltered reedings chemical analysis	Calcite <sup>a</sup> , gypsum <sup>d</sup> , aluminosilicates <sup>d</sup> , oxalates <sup>e</sup>		Calcite <sup>a</sup> , oxalates <sup>e</sup> , gypsum <sup>f</sup>		Calcite <sup>a</sup> , gypsum <sup>d</sup> , aluminosilicates <sup>e</sup> , oxalates <sup>e</sup>			
Unsheltered flutings	13.67 (1.14)	3.55 (0.67)	1.83 (0.31)	0.67 (0.23)				
Unsheltered flutings chemical analysis	Calcite <sup>b</sup> , aluminosilicates <sup>e</sup> , gypsum <sup>d</sup> , oxalates <sup>e</sup> , organic compounds <sup>e</sup>		Calcite <sup>a</sup> , aluminosilicates <sup>d</sup> , organic compounds <sup>e</sup>					
Unsheltered reedings	7.28 (0.84)	11.44 (1.04)	3.61 (0.60)	2.33 (0.51)			(0.22)	(0.04) 0
Unsheltered reedings chemical analysis	Calcite <sup>b</sup> , aluminosilicates <sup>e</sup> , gypsum <sup>d</sup> , oxalates <sup>e</sup> , barite <sup>e</sup> , organic compounds <sup>e</sup>		Calcite <sup>a</sup> , aluminosilicates <sup>e</sup> , organic compounds <sup>e</sup>				Calcite <sup>a</sup> , aluminosilicates <sup>e</sup> , organic compounds <sup>e</sup>	
Partially cleaned surface	17.96 (8.62)	15.43 (6.93)					1.00 (0.63)	3.45 (1.14)
Partially cleaned surface chemical analysis	Calcite <sup>b</sup> , aluminosilicates <sup>d</sup> , gypsum <sup>d</sup> , oxalates <sup>e</sup> ,						Calcite <sup>b</sup> , aluminosilicates <sup>e</sup> , oxalates <sup>e</sup>	

The results derived by the chemical analyses of the same surfaces are also provided.

<sup>a</sup> >75%.

<sup>b</sup> 50–75%.

<sup>c</sup> 20–50%.

<sup>d</sup> 5–20%.

<sup>e</sup> <1–5%.

<sup>f</sup> <1% (traces).

<sup>1</sup> Prior to any treatment.

<sup>2</sup> Ion-exchange resin-paste with deionized water.

<sup>3</sup> Biological paste.

<sup>4</sup> Wet micro-blasting method.

Table 2  
Mean percentage of the studied surface covered by black particles

	Diagnosis	BP	Ds (30 min)	DS (60 min)	WMB
Sheltered flutings	3.75	0.04		0.45	0.04
Sheltered readings	1.73	0.05		0.06	
Unsheltered flutings	0.53		0.04		
Unsheltered readings	0.29		0.04		0.02
Crust partially cleaned – WMB	0.57				0.04

capable of eliminating the number of black particles. In contrast, the WMB method demonstrates a greater efficiency in diminishing the black and white particles, which is in accordance with the results of the chemical analysis [13,14].

Table 2 depicts the percentage of surface covered by black particles in the same cases as in Table 1 and reveals that the chemical cleaning methods achieve considerable elimination of black particles. The effect of cleaning is reflected by the MFD algorithm through the drastic reduction of decay areas on the chemically processed surfaces. Comparison of the cleaning techniques indicates that the DS method is less able of diminishing the percentage of the surface covered by black crusts. Table 2 provides the coverage of the decay areas which is in close agreement with the number of the MFD detected decay particles on the studied surfaces.

Another interesting quantitative measure concerns the size distribution of decay particles, as summarized in Table 3. The distribution in terms of the median (robust) measure rather than its mean measure is presented, since the actual size distribution on several images tested is heavily tailed. In particular, the measures computed are defined as follows:

- *Median*: The particle size that is greater than the 50% of the sizes detected on the image.
- *Lower and upper quartiles*: The particle sizes that are greater than 25% and 75% of sizes detected on the image, respectively.

The results reported in Table 3 indicate that the size distribution of black particles encountered on flutings is spread to greater values than the size distribution of black particles detected on readings. This observation holds true for the surfaces located both on sheltered and unsheltered areas. The above assessment is quite reasonable, since flutings function as areas of pollutant accumulation, while readings represent more washed-out areas [13,14].

Up to this point, we consider only area measurements on the detected decay patterns. Intensity information from the original image on these patterns is also of great

Table 3  
Size distribution of decay patterns encountered on surfaces of different exposure

	Lower quartile	Median	Upper quartile
Sheltered flutings	10	18	27
Sheltered readings	8	13	21
Unsheltered flutings	9	14	23
Unsheltered readings	9	12	19

concern, since it relates with the depth of the crust accumulated on the surface. In this study, the aspect of crust thickness is approached in a rather qualitative point of view in that darker formations imply more light absorption and, thus, thicker formation of black crust. Since the intensity distribution does not reflect heavy tails and resembles better the normal distribution, the reported measures reflect the mean, upper and lower quartiles of the distribution over the particles of all images of the same type considered.

The results presented in Table 4 reveal several issues that can be studied through intensity distributions. First, it indicates the change in intensity distribution before and after chemical cleaning on sheltered flutings. Then it reveals the effects of exposure as reflected to intensity levels. Finally, it summarizes the effect of cleaning in intensity distributions from the same piece of material (partially cleaned). It is verified that the MFD approach derives intensity distributions shifted to lower values when applied to surfaces with black crusts of higher thickness (sheltered flutings). Moreover, after chemical cleaning the intensity distribution of the detected particles is increased, since such areas are diminished and appear brighter and less disturbing in a macroscopic point of view. This result also indicates that even though chemical cleaning does not completely eliminate all decay products, it manages to reduce the thickness of the remaining crust patterns relative to their original state.

Comparing the quantitative results in Table 1 with the results of chemical analyses in each case, we can further explain and validate the performance of the algorithm in

Table 4  
Intensity distributions of black particles detected at various surfaces

	Lower quartile	Mean intensity	Upper quartile
<i>Effect of cleaning on sheltered flutings</i>			
Sheltered flutings – diagnosis	41.50	53.22	66.00
Sheltered flutings – DS	41.50	59.37	73.00
Sheltered flutings – BP	61.00	68.20	77.00
Sheltered flutings – WMB	78.33	66.07	103.33
<i>Effect of exposure</i>			
Sheltered flutings – diagnosis	41.50	53.22	66.00
Sheltered readings	85.00	95.97	107.00
Unsheltered flutings	90.00	96.31	104.00
Unsheltered readings	100.00	110.33	122.00
<i>Consideration on the partially cleaned surface of Fig. 6</i>			
Partially cleaned surface – diagnosis	77	85.92	88
Partially cleaned surface – WMB	97	102.83	107

terms of the chemical composition of the decay effects. For example, the increased number of black and white particles in diagnoses compared to cleaned surfaces is mainly due to the increased concentration of decay products, such as aluminosilicates and gypsum. Furthermore, the increased number of black particles in untreated sheltered flutings and readings compared to the unsheltered ones is due to the increased concentration of gypsum and aluminosilicates relevant to the concentration of black particles.

## 5. Conclusions

In this paper we explore the potential of non-destructive inspection for assessing environmental damage and evaluating the effect of cleaning on stone monuments. We introduce the so-called “Morphologically Fused Detection (MFD)” technique for non-destructive detection and segmentation of deterioration patterns on marble surfaces. Its design aims at localizing the decay areas while preserving their shape and extent. The proposed MFD approach employs the conditional thickening operator to combine and fuse the results of two individual detectors, i.e. a Gaussian and a morphological detector, as to take advantage of the strong points of each one of them.

The application areas of the proposed method include the evaluation of decay patterns on surfaces and the tracking of the decay process in the course of time, the assessment of the effects of various cleaning methods on the stone surface and the ability to compare the performances of several cleaning methods in terms of their effectiveness in removing black and white crusts. The set of images used to test the diagnostic procedure are obtained with the aid of a Fiber Optics Microscope Monitoring System, which provides reliable information about the texture of the stone. The images tested depict the degradation state on areas of the monument under different conditions of environmental exposure. The deterioration patterns detected by the proposed approach are distinguished into two broad categories, defined as “black particles” and “white particles”, respectively. This discrimination is associated with the chemical composition of the deterioration patterns.

The detection and segmentation of deterioration patterns provide the means for defining qualitative and quantitative measures associated with decay effects. As it is assessed by the derived results, the numbers of the black and white particles are significantly eliminated after the application of chemical cleaning. More explicitly, the employed MFD approach can discriminate the efficiency of the cleaning methods and reveals that WMB cleaning can effectively remove the majority of black and white particles. Furthermore, it is verified that degradation patterns encountered on sheltered flutings are more in number and larger in spatial extent than those detected on sheltered readings or unsheltered flutings. This assessment is readily explained by the formation mechanism of black crusts. Finally, the proposed non-destructive approach enables measurements on the intensity distribution of decay, which

is directly associated with the thickness of the crusts at these areas. This study further demonstrates the potential of employing the MFD approach to monitor, in a non-destructive way, the decay rate of exposed stone.

Future research efforts on evaluating corrosion damage could be extended towards recording and classifying degraded areas prevailing on surfaces of different exposure and or/cleaning conditions. This work indicated that characteristic features that could be used for such a purpose include the size of decay areas, the intensity distribution within the segmented areas and their spatial arrangement. Furthermore, features related to the morphology of spots, such as boundary moments, orientation, roughness, eccentricity, and bending energy of the boundary are also of considerable importance. The classification process could be realized effectively based on fuzzy algorithms [19,20] that can handle the peculiarities and uncertainties on the distribution of these features.

## Acknowledgement

The authors would like to acknowledge the anonymous reviewers for their valuable comments.

## References

- [1] Moropoulou A, Bisbikou K, Torfs K, Van Grieken R, Zezza F, Macri F. Origin and growth of weathering crusts on ancient marbles in industrial atmosphere. *Atmos Environ* 1998;32:967–82.
- [2] Cammufo D. Acidification and its policy implications. Amsterdam: Elsevier; 1986.
- [3] Jimenez SC. Deposition of airborne organic pollutants on historic buildings. *Atmos Environ* 1993;B27:77–85.
- [4] Lebrun V, Bonino E, Nivart JF, Pirard E. Development of specific acquisition techniques for field imaging-applications to outcrops and marbles. In: Proceedings of the international symposium of geovision on imaging applications in geology. Liege, Belgium; 1999. p. 165–8.
- [5] Pappas M, Pitas I. Old painting digital color restoration. In: Noblesse workshop on non-linear model based image analysis. Glasgow, Scotland; 1998. p. 188–92.
- [6] Cardell C, Yebra A, Van Grieken R. Applying digital image processing to SEM-EDX and BSE images to determine and quantify porosity and salts with depth in porous media. *Microchim Acta* 2002;140(1-2):9–14.
- [7] Moltedo L, Mortelliti G, Salvetti O, Vitulano D. Computer aided analysis of buildings. *J Cult Herit* 2000;1(1):59–67.
- [8] Boukouvalas C, De Natale F, De Toni G, Kittler J, Marik R, Mirmehdi M, Petrou M, Le Roy P, Salgari R, Vernazza G. ASSIST: automatic system for surface inspection and sorting of tiles. *J Mater Process Technol* 1998;82(1-3):179–88.
- [9] Shen L, Rangayyan RM. Detection and classification of mammographic calcifications. *Int J Pattern Recogn Art Intel* 1993;7(6): 1403–16.
- [10] Rapantzikos K, Zervakis M. Nonlinear enhancement and segmentation algorithm for the detection of age-related macular degeneration (AMD) in human eye's retina. In: Proceedings of the international conference on image processing. Thessaloniki, Greece; 2001. p. 1055–8.
- [11] Salfity MF, Kaufmann GH, Granitto P, Ceccatto HA. A computer-aided diagnosis for automated detection and classification of clustered microcalcifications in mammograms. In: Proceedings of the third simposio argentino de informática en Salud; 2000. p. 41–7.

- [12] Dengler J, Behrens S, Desaga JF. Segmentation of micro-calcifications in mammograms. *IEEE Trans Medical Imaging* 1993;12: 634–42.
- [13] Moropoulou A, Kouli M, Delegou ET, Bakolas A, Karoglou M, Rapti E, Kouris S, Mauridis Th, Ypsilanti E, Avdelidis NP, Ntae D. Conservation interventions planning for the main façade of the National Archaeological Museum. In: Final research working paper, Lab of Materials Science and Engineering, National Technical University of Athens; August 2002.
- [14] Kouli M, Delegou ET, Dai D, Rapti E, Mavridis T, Moropoulou A. FTIR for the assessment of cleaning interventions on pentelic marble surfaces. In: Sixth international symposium on the conservation of monuments in the mediterranean basin. Lisbon, CD-Rom Proc.; 2004.
- [15] Moropoulou A, Tsiourva Th, Bisbikou K, Tsantila V, Biscontin G, Longega G, Groggia M, Dalaklis E, Petritaki A. Evaluation of cleaning procedures on the facades of the Bank of Greece historical building in the center of Athens. *Build Environ* 2002; 37:753–60.
- [16] Maravelaki-Kalaitzaki P. Characterization of weathering crusts from monuments in Athens, Greece, In: Taylor and Francis Group, editors. Proceedings of international workshop on air pollution and cultural heritage. Balkema, London; 2004. p. 71–8.
- [17] Sabioni C. Contribution of atmospheric deposition to the formation of damage layers. *Sci Total Environ* 1995;167:49–55.
- [18] Li H, Ray Lui KJ, Lo SB. Fractal modeling and segmentation for the enhancement of micro-calcifications in digital mammograms. *IEEE Trans Medical Imaging* 1997;16:785–98.
- [19] Betanzos Alonso A, Varela Arcay B, Martinez Castro A. Analysis and evaluation of hard and fuzzy clustering segmentation techniques in burned patient images. *Image Vis Comput* 2000;18:1045–54.
- [20] Tsekouras G, Sarimveis B, Kavaklia E, Bafas G. A hierarchical fuzzy-clustering approach to fuzzy modeling. *Fuzzy Sets Syst* 2005;150: 245–66.